Mathematical and Computational Applications

MDPI

Article

Sierpiński Fractals and the Dimension of Their Laplacian Spectrum †

Mark Pollicott * and Julia Slipantschuk *

Department of Mathematics, University of Warwick, Coventry CV4 7AL, UK
* Correspondence: masdbl@warwick.ac.uk (M.P.); julia.slipantschuk@warwick.ac.uk (J.S.)
† Dedicated to Károly Simon on the occasion of their 60+1st birthday.

Abstract: We establish rigorous estimates for the Hausdorff dimension of the spectra of Laplacians associated with Sierpiński lattices and infinite Sierpiński gaskets and other post-critically finite self-similar sets.

Keywords: Laplacian spectrum; Sierpiński Fractals; Hausdorff dimension; transfer operator; Lagrange-Chebyshev interpolation

MSC: 28A80; 37F35; 37C30; 65D05

1. Introduction

The study of the Laplacian on manifolds has been a very successful area of mathematical analysis for over a century, combining ideas from topology, geometry, probability theory and harmonic analysis. A comparatively new development is the theory of a Laplacian for certain types of naturally occurring fractals, see [1–7], to name but a few. A particularly well-known example is the following famous set.

Definition 1. *The* Sierpiński triangle $\mathcal{T} \subset \mathbb{R}^2$ *(see Figure 1a) is the smallest non-empty compact set such that* $\bigcup_{i=1}^{3} T_i(\mathcal{T}) = \mathcal{T}$ *where* $T_1, T_2, T_3 \colon \mathbb{R}^2 \to \mathbb{R}^2$ *are the affine maps*

$$T_1(x,y) = \left(\frac{x}{2}, \frac{y}{2}\right) \qquad T_2(x,y) = \left(\frac{x}{2} + \frac{1}{2}, \frac{y}{2}\right)$$
$$T_3(x,y) = \left(\frac{x}{2} + \frac{1}{4}, \frac{y}{2} + \frac{\sqrt{3}}{4}\right).$$

In the literature, this set is also often referred to as the Sierpiński gasket, *and denoted* SG_2.

A second object which will play a role is the following infinite graph:

Definition 2. *Let* $V_0 = \{(0,0), (1,0), (\frac{1}{2}, \frac{\sqrt{3}}{2})\}$ *be the set of vertices of* $\mathcal{T}$ *and define* $V_n = \bigcup_{i=1}^{3} T_i(V_{n-1})$. *Furthermore, fix a sequence* $\omega = (\omega_n)_{n\in\mathbb{N}} \subset \{1,2,3\}^{\mathbb{N}}$, *and let*

$$V^{\infty} = \bigcup_{i=1}^{\infty} V^n \text{ with } V^n = T_{\omega_1}^{-1} \circ \cdots \circ T_{\omega_n}^{-1}(V_n),$$

where we use the inverses

$$T_1^{-1}(x,y) = (2x, 2y) \qquad T_2^{-1}(x,y) = (2x-1, 2y)$$
$$T_3^{-1}(x,y) = \left(2x - \frac{1}{2}, 2y - \frac{\sqrt{3}}{2}\right).$$

Citation: Pollicott, M.; Slipantschuk, J. Sierpiński Fractals and the Dimension of Their Laplacian Spectrum. *Math. Comput. Appl.* **2023**, *28*, 70. https://doi.org/10.3390/mca28030070

Academic Editors: István Kolossváry, Roland Molontay and Michał Rams

Received: 5 January 2023
Revised: 27 April 2023
Accepted: 28 April 2023
Published: 17 May 2023

The definition of V^∞ depends on the choice of ω; however, as will be explained below, the relevant results do not, allowing us to omit the dependence in our notation. The points in V^∞ correspond to the vertices of an infinite graph $\mathcal{L}$ called a Sierpiński lattice, *for which the edges correspond to pairs of vertices (v, v'), with $v, v' \in V^\infty$ such that $\|v - v'\|_2 = 1$ (see Figure 1b). Equivalently, $\mathcal{L}$ has an edge (v, v') if and only if*

$$v, v' \in T_{\omega_1}^{-1} \circ \cdots \circ T_{\omega_n}^{-1} \circ T_{i_n} \circ \cdots \circ T_{i_1}(V_0)$$

for some $i_1, \ldots, i_n \in \{1, 2, 3\}$, $n \geqslant 0$.

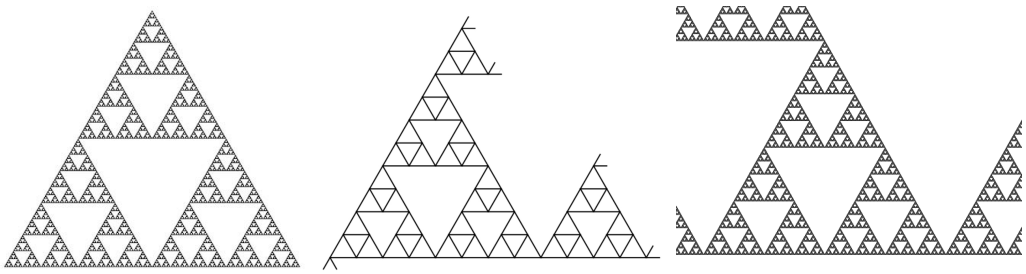

(a) **(b)** **(c)**

Figure 1. (**a**) The standard Sierpiński triangle $\mathcal{T}$; (**b**) The Sierpiński lattice $\mathcal{L}$; and (**c**) The infinite Sierpiński triangle $\mathcal{T}^\infty$.

Finally, we will also be interested in infinite Sierpiński gaskets, which can be defined similarly to Sierpiński lattices as follows.

Definition 3. *For a fixed sequence $\omega = (\omega_n)_{n \in \mathbb{N}}$, we define an* infinite Sierpiński gasket *to be the unbounded set $\mathcal{T}^\infty$ given by*

$$\mathcal{T}^\infty = \bigcup_{n=0}^{\infty} \mathcal{T}^n, \text{ with } \mathcal{T}^n = T_{\omega_1}^{-1} \circ \cdots \circ T_{\omega_n}^{-1}(\mathcal{T}),$$

which is a countable union of copies of the standard Sierpiński triangle $\mathcal{T}$ (see Figure 1c). As for Sierpiński lattices, the definition of $\mathcal{T}^\infty$ depends on the choice of ω, but we omit this dependence in our notation as the cited results hold independently of it.

The maps T_1, T_2 and T_3 are similarities on $\mathbb{R}^2$ with respect to the Euclidean norm, and more precisely

$$\|T_i(x_1, y_1) - T_i(x_2, y_2)\|_2 = \frac{1}{2}\|(x_1, y_1) - (x_2, y_2)\|_2$$

for $(x_1, y_1), (x_2, y_2) \in \mathbb{R}^2$ and $i = 1, 2, 3$, and thus by Moran's theorem the Hausdorff dimension of $\mathcal{T}$ has the explicit value $\dim_H(\mathcal{T}) = \frac{\log 3}{\log 2}$ [8]. We can easily give the Hausdorff dimensions of the other spaces. It is clear that $\dim_H(\mathcal{L}) = 1$, and since an infinite Sierpiński gasket $\mathcal{T}^\infty$ consists of countably many copies of $\mathcal{T}$, it follows that we also have $\dim_H(\mathcal{T}^\infty) = \frac{\log 3}{\log 2}$.

In this note, we are concerned with other fractal sets closely associated with the infinite Sierpiński gasket $\mathcal{T}^\infty$ and the Sierpiński lattice $\mathcal{L}$, for which the Hausdorff dimensions are significantly more difficult to compute.

In Section 2, we will describe how to associate to $\mathcal{T}$ a Laplacian $\Delta_\mathcal{T}$ which is a linear operator defined on suitable functions $f : \mathcal{T} \to \mathbb{R}$. An eigenvalue $\lambda \geqslant 0$ for $-\Delta_\mathcal{T}$ on the Sierpiński triangle is then a solution to the basic identity

$$\Delta_\mathcal{T} f + \lambda f = 0.$$

The spectrum $\sigma(-\Delta_{\mathcal{T}}) \subset \mathbb{R}^+$ of $-\Delta_{\mathcal{T}}$ is a countable set of eigenvalues. In particular, its Hausdorff dimension satisfies $\dim_H(\sigma(-\Delta_{\mathcal{T}})) = 0$. A nice account of this theory appears in the survey note of Strichartz [6] and their book [9].

By contrast, in the case of the infinite Sierpiński gasket and the Sierpiński lattice, there are associated Laplacians, denoted $\Delta_{\mathcal{T}^\infty}$ and $\Delta_{\mathcal{L}}$, respectively, with spectra $\sigma(-\Delta_{\mathcal{T}^\infty}) \subset \mathbb{R}^+$ and $\sigma(-\Delta_{\mathcal{L}}) \subset \mathbb{R}^+$, which are significantly more complicated. In particular, their Hausdorff dimensions are non-zero and therefore their numerical values are of potential interest. However, unlike the case of the dimensions of the original sets $\mathcal{T}^\infty$ and $\mathcal{L}$, there is no clear explicit form for this quantity. Fortunately, using thermodynamic methods we can estimate the Hausdorff dimension (which in this case equals the Box counting dimension, as will become apparent in the proof) numerically to very high precision.

Theorem 1. *The Hausdorff dimension of* $\sigma(-\Delta_{\mathcal{T}^\infty})$ *and* $\sigma(-\Delta_{\mathcal{L}})$ *satisfy*

$$\dim_H(\sigma(-\Delta_{\mathcal{T}^\infty})) = \dim_H(\sigma(-\Delta_{\mathcal{L}})) = 0.55161856837246\ldots$$

A key point in our approach is that we have rigorous bounds, and the value in the above theorem is accurate to the number of decimal places presented. We can actually estimate this Hausdorff dimension to far more decimal places. To illustrate this, in the final section we give an approximation to 100 decimal places.

It may not be immediately evident what practical information the numerical value of the Hausdorff dimension gives about the sets $\mathcal{T}^\infty$ and $\mathcal{L}$ but it may have the potential to give an interesting numerical characteristic of the spectra. Beyond pure fractal geometry, the spectra of Laplacians on fractals are also of practical interest, for instance in the study of vibrations in heterogeneous and random media, or the design of so-called fractal antennas [10,11].

We briefly summarize the contents of this note. In Section 2 we describe some of the background for the Laplacian on the Sierpiński graph. In particular, in Section 2.3 we recall the basic approach of *decimation* which allows $\sigma(\Delta_{\mathcal{T}})$ to be expressed in terms of a polynomial $R_{\mathcal{T}}(x)$. Although we are not directly interested in the zero-dimensional set $\sigma(-\Delta_{\mathcal{T}})$, the spectra $\sigma(-\Delta_{\mathcal{T}^\infty})$ and $\sigma(-\Delta_{\mathcal{L}})$ actually contain a Cantor set $\mathcal{J}_{\mathcal{T}} \subset [0,5]$, the so-called Julia set associated with the polynomial $R_{\mathcal{T}}(x)$.

As one would expect, other related constructions of fractal sets have similar spectral properties and their dimension can be similarly studied. In Section 3 we consider higher-dimensional Sierpiński simplices, post-critically finite fractals, and an analogous problem where we consider the spectrum of the Laplacian on infinite graphs (e.g., the Sierpiński graph and the Pascal graph). In Section 4, we recall the algorithm we used to estimate the dimension and describe its application. This serves to both justify our estimates and also to use them as a way to illustrate a method with wider applications.

2. Spectra of the Laplacians

2.1. Energy Forms

There are various approaches to defining the Laplacian $\Delta_{\mathcal{T}}$ on $\mathcal{T}$. We will use one of the simplest ones, using energy forms.

Following Kigami [2], the definition of the spectrum of the Laplacian for the Sierpiński gasket $\mathcal{T}$ involves a natural sequence of finite graphs X_n with

$$X_0 \subset X_1 \subset X_2 \subset \cdots \subset \bigcup_n X_n \subset \overline{\bigcup_n X_n} =: \mathcal{T},$$

the first three of which are illustrated in Figure 2. To this end, let

$$V_0 = \left\{(0,0), (1,0), \left(\frac{1}{2}, \frac{\sqrt{3}}{2}\right)\right\}$$

be the three vertices of X_0. The vertices of X_n can be defined iteratively to be the set of points satisfying

$$V_n = T_1(V_{n-1}) \cup T_2(V_{n-1}) \cup T_3(V_{n-1}) \quad \text{for } n \geqslant 1.$$

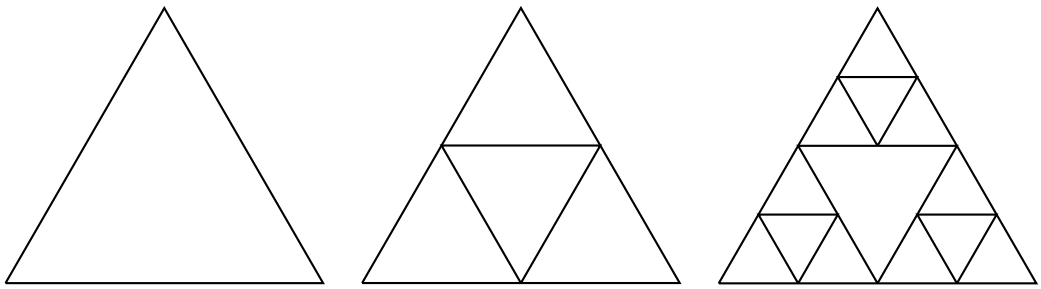

Figure 2. The first three graphs for the Sierpiński triangle.

We denote by $\ell^2(V_n)$ (for $n \geqslant 0$) the real valued functions $f\colon V_n \to \mathbb{R}$ (where the ℓ^2 notation is used for consistency with the infinite-dimensional case despite having no special significance for finite sets).

Definition 4. *To each of the finite graphs X_n ($n \geqslant 0$) we can associate bilinear forms $\mathcal{E}_n\colon \ell^2(V_n) \times \ell^2(V_n) \to \mathbb{R}$ called* self-similar energy forms *given by*

$$\mathcal{E}_n(f,g) = c_n \sum_{x \sim_n y} (f(x) - f(y))(g(x) - g(y)), \tag{1}$$

where $x, y \in V_n$ are vertices of X_n, and $x \sim_n y$ denotes neighboring edges in X_n. In particular, $x \sim_n y$ precisely when there exists $x', y' \in V_{n-1}$ and $i \in \{1,2,3\}$ such that $x = T_i(x')$ and $y = T_i(y')$. The value $c_n > 0$ denotes a suitable scaling constant. With a slight abuse of notation, we also write $\mathcal{E}_n(f) := \mathcal{E}_n(f,f)$ for the corresponding quadratic form $\ell^2(V_n) \to \mathbb{R}$.

To choose the values $c_n > 0$ (for $n \geqslant 0$), we want the sequence of bilinear forms $(\mathcal{E}_n)_{n=0}^{\infty}$ to be consistent by asking that for any $f_{n-1}\colon V_{n-1} \to \mathbb{R}$ (for $n \geqslant 1$) we have

$$\mathcal{E}_{n-1}(f_{n-1}) = \mathcal{E}_n(f_n),$$

where $f_n\colon V_n \to \mathbb{R}$ denotes an extension which satisfies

(a) $f_n(x) = f_{n-1}(x)$ for $x \in V_{n-1}$; and
(b) f_n satisfying (a) minimizes $\mathcal{E}_n(f_n)$ (i.e., $\mathcal{E}_n(f_n) = \min_{f \in \ell^2(V_n)} \mathcal{E}_n(f)$).

The following is shown in [9], for example.

Lemma 1. *The family $(\mathcal{E}_n)_{n=0}^{\infty}$ is consistent if we choose $c_n = \left(\frac{5}{3}\right)^n$ in (1).*

The proof of this lemma is based on solving families of simultaneous equations arising from (a) and (b). We can now define a bilinear form for functions on $\mathcal{T}$ using the consistent family of bilinear forms $(\mathcal{E}_n)_{n=0}^{\infty}$.

Definition 5. *For any continuous function $f\colon \mathcal{T} \to \mathbb{R}$ we can associate the limit*

$$\mathcal{E}(f) := \lim_{n \to +\infty} \mathcal{E}_n(f) \in [0, +\infty]$$

and let $\mathrm{dom}(\mathcal{E}) = \{f \in C(\mathcal{T}) : \mathcal{E}(f) < +\infty\}$.

Remark 1. *We can consider eigenfunctions $f \in \mathrm{dom}(\mathcal{E})$ which satisfy Dirichlet boundary conditions (i.e., $f|V_0 = 0$).*

2.2. Laplacian for $\mathcal{T}$

To define the Laplacian $\Delta_{\mathcal{T}}$, the last ingredient is to consider an inner product defined using the natural measure μ on the Sierpiński triangle $\mathcal{T}$.

Definition 6. *Let μ be the natural measure on $\mathcal{T}$ such that*

$$\mu\big(T_{i_1} \circ \cdots \circ T_{i_n}\mathrm{co}(V_0)\big) = \frac{1}{3^n} \quad \text{for } i_1, \ldots, i_n \in \{1,2,3\},$$

where $\mathrm{co}(V_0)$ is the convex hull of V_0, i.e., the filled-in triangle.

In particular, μ is the Hausdorff measure for $\mathcal{T}$, and the unique measure on $\mathcal{T}$ for which

$$T_i^*\mu = \frac{1}{3}\mu \quad \text{for } i = 1,2,3.$$

The subspace $\mathrm{dom}(\mathcal{E}) \subset L^2(\mathcal{T},\mu)$ is a Hilbert space. Using the measure μ and the bilinear form $\mathcal{E}$, we recall the definition of the Laplacian $\Delta_{\mathcal{T}}$.

Definition 7. *For $u \in \mathrm{dom}(\mathcal{E})$ which vanishes on V_0 we can define the Laplacian to be a continuous function $\Delta_{\mathcal{T}}u\colon \mathcal{T} \to \mathbb{R}$ such that*

$$\mathcal{E}(u,v) = -\int (\Delta_{\mathcal{T}}u)v d\mu$$

for any $v \in \mathrm{dom}(\mathcal{E})$.

Remark 2. *For each finite graph X_n, the spectrum $\sigma(-\Delta_{X_n})$ for the graph Laplacian Δ_{X_n} will consist of a finite number of solutions of the eigenvalue equation*

$$\Delta_{X_n} f + \lambda f = 0. \tag{2}$$

This is easy to see because V_n is finite and thus the space $\ell^2(V_n)$ is finite-dimensional and so the graph Laplacian can be represented as a matrix. There is then an alternative pointwise formulation of the Laplacian of the form

$$\Delta_{\mathcal{T}}u(x) = \frac{3}{2}\lim_{n\to+\infty} 5^n \Delta_{X_n}u(x) \tag{3}$$

where $x \in \bigcup_{n=1}^{\infty} V_n \setminus V_0$. The eigenvalue equation $\Delta_{\mathcal{T}}u + \lambda u = 0$ then has admissible solutions provided $u, \Delta_{\mathcal{T}}u \in C(\mathcal{T})$. A result of Kigami is that $u \in \mathrm{dom}(\mathcal{E})$ if and only if the convergence in (3) is uniform [12].

2.3. Spectral Decimation for $\sigma(-\Delta_{\mathcal{T}})$

We begin by briefly recalling the fundamental notion of spectral decimation introduced by [3,13,14], which describes the spectrum $\sigma(-\Delta_{\mathcal{T}})$.

Definition 8. *Given the polynomial $R_{\mathcal{T}}\colon [0,5] \to \mathbb{R}$ defined by*

$$R_{\mathcal{T}}(x) = x(5-x),$$

we can associate local inverses (see Figure 3) $S_{-1,\mathcal{T}}, S_{+1,\mathcal{T}}\colon [0,5] \to [0,5]$ of the form

$$S_{\epsilon,\mathcal{T}}(x) = \frac{5}{2} + \frac{\epsilon}{2}\sqrt{25-4x} \quad \text{for } \epsilon = \pm 1. \tag{4}$$

The process of spectral decimation (see Section 3.2 in [9], or [1]) describes the eigenvalues of $-\Delta_{\mathcal{T}}$ as renormalized limits of (certain) eigenvalue sequences of $-\Delta_{X_n}, n \in \mathbb{N}$. These eigenvalues, essentially, follow the recursive equality $\lambda_{n+1} = S_{\pm 1,\mathcal{T}}(\lambda_n)$, while the corresponding eigenfunctions of $-\Delta_{X_{n+1}}$ are such that their restrictions to V_n are eigenfunctions for $-\Delta_{X_n}$. Thus, the eigenvalue problem can be solved inductively, constructing solutions f to the eigenvalue equation (2) at level $n+1$ from solutions at level $n \in \mathbb{N}$. The values of f at vertices in $V_{n+1} \setminus V_n$ are obtained from solving the additional linear equations that arise from the eigenvalue equation $\Delta_{X_{n+1}} f + \lambda f = 0$, which allows for exactly two solutions. The exact limiting process giving rise to eigenvalues of $-\Delta_{\mathcal{T}}$ is described by the following result.

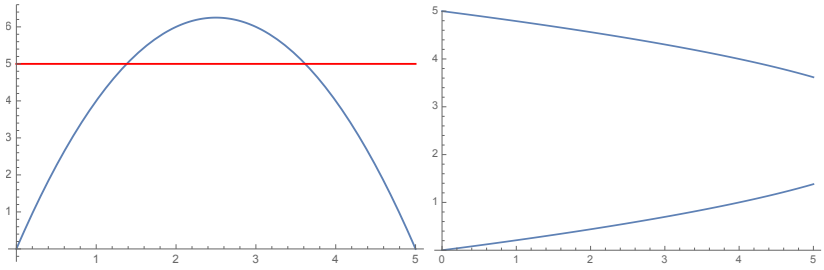

Figure 3. The polynomial $R_{\mathcal{T}}(x)$ and the contracting inverse branches $S_{-1,\mathcal{T}}$ and $S_{+1,\mathcal{T}}$ for the Sierpiński triangle $\mathcal{T}$.

Proposition 1 ([1,3,15]). *Every solution $\lambda \in \mathbb{R}$ to the eigenvalue equation*

$$\Delta_{\mathcal{T}} u + \lambda u = 0 \tag{5}$$

can be written as

$$\lambda = \frac{3}{2} \lim_{m \to +\infty} 5^{m+c} \lambda_m, \tag{6}$$

for a sequence $(\lambda_m)_{m \geqslant m_0}$ and a positive integer $c \in \mathbb{N}_0$ satisfying

1. *$\lambda_{m_0} = 2$ and $c = 0$, or $\lambda_{m_0} = 5$ and $c \geqslant 1$, or $\lambda_{m_0} = 3$ and $c \geqslant 2$;*
2. *$\lambda_m = \lambda_{m+1}(5 - \lambda_{m+1}) = R_{\mathcal{T}}(\lambda_{m+1})$ for all $m \geqslant m_0$; and*
3. *the limit (6) is finite.*

Conversely, the limit of every such sequence gives rise to a solution of (5).

We remark that, equivalently, the sequence $(\lambda_m)_{m \geqslant m_0}$ could be described recursively as $\lambda_{m+1} = S_{\epsilon_m,\mathcal{T}}(\lambda_m)$ where $\epsilon_m \in \{\pm 1\}$ for $m \geqslant m_0$. The finiteness of the limit (6) is equivalent to there being an $m' \geqslant m_0$ such that $\epsilon_m = -1$ for all $m \geqslant m'$.

2.4. Spectrum of the Laplacian for Sierpiński Lattices

For a Sierpiński lattice, we define the Laplacian $\Delta_{\mathcal{L}}$ by

$$(\Delta_{\mathcal{L}} f)(x) = s_x \sum_{y \sim x} (f(y) - f(x))$$

with

$$s_x = \begin{cases} 2 & \text{if } x \text{ is a boundary point,} \\ 1 & \text{if } x \text{ is not a boundary point,} \end{cases}$$

which is a well-defined and bounded operator from $\ell^2(V^\infty)$ to itself (this follows from the fact that each vertex of $\mathcal{L}$ has at most 4 neighbors).

Remark 3. *We note that our definition of V^∞ and $\mathcal{L}$ depended on the choice of a sequence $(\omega_n)_{n \in \mathbb{N}}$, and graphs resulting from different sequences are typically not isometric ([7], Lemma 2.3(ii)).*

On the other hand, the spectrum $\sigma(-\Delta_{\mathcal{L}})$ turns out to be independent of this choice (see [7], Remark 4.2 or [4], Proposition 1).

The operator $-\Delta_{\mathcal{L}}\colon \ell^2(V^\infty) \to \ell^2(V^\infty)$ has a more complicated spectrum which depends on the following definition.

Definition 9 (cf. [8]). *We define the Julia set associated with $R_{\mathcal{T}}$ to be the smallest non-empty closed set $\mathcal{J}_{\mathcal{T}} \subset [0,5]$ such that*

$$\mathcal{J}_{\mathcal{T}} = S_{-1,\mathcal{T}}(\mathcal{J}_{\mathcal{T}}) \cup S_{+1,\mathcal{T}}(\mathcal{J}_{\mathcal{T}}).$$

This leads to the following description of the spectrum $\sigma(-\Delta_{\mathcal{L}})$.

Proposition 2 ([7], Theorem 2). *The operator $-\Delta_{\mathcal{L}}$ on $\ell^2(V^\infty)$ is bounded, non-negative and self-adjoint and has spectrum*

$$\sigma(-\Delta_{\mathcal{L}}) = \mathcal{J}_{\mathcal{T}} \cup \left(\{6\} \cup \bigcup_{n=0}^{\infty} R^{-n}(\{3\}) \right).$$

This immediately leads to the following.

Corollary 1. *We have that* $\dim_H(\sigma(-\Delta_{\mathcal{L}})) = \dim_H(\mathcal{J}_{\mathcal{T}})$.

Thus, estimating the Hausdorff dimension of the spectrum $\sigma(-\Delta_{\mathcal{L}})$ is equivalent to estimating that of the Julia set $\mathcal{J}_{\mathcal{T}}$. The following provides a related application.

Example 1 (Pascal graph). *Consider the Pascal graph $\mathcal{P}$ [16], which is an infinite 3-regular graph, see Figure 4. Its edges graph is the Sierpiński lattice $\mathcal{L}$, and as was shown by Quint [16], the spectrum $\sigma(-\Delta_{\mathcal{P}})$ of its Laplacian $-\Delta_{\mathcal{P}}$ is the union of a countable set and the Julia set of a certain polynomial (affinely) conjugated to $R_{\mathcal{T}}$. From this, we deduce that*

$$\dim_H(\sigma(-\Delta_{\mathcal{P}})) = \dim_H(\mathcal{J}_{\mathcal{P}}) = \dim_H(\mathcal{J}_{\mathcal{L}}) = \dim_H(\sigma(-\Delta_{\mathcal{L}})),$$

which we estimate in Theorem 1.

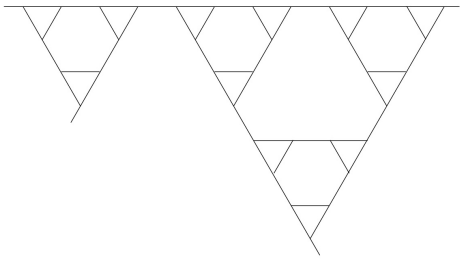

Figure 4. The Pascal graph.

2.5. Spectrum of the Laplacian for Infinite Sierpiński Gaskets

We finally turn to the case of an infinite Sierpiński gasket $\mathcal{T}^\infty$. The Laplacian $\Delta_{\mathcal{T}^\infty}$ is an operator with a domain in $L^2(\mathcal{T}^\infty, \mu^\infty)$. Here, μ^∞ is the natural measure on $\mathcal{T}^\infty$, whose restriction to $\mathcal{T}$ equals μ, and such that any two isometric sets are of equal measure (see [7]).

Remark 3 applies almost identically also to the Sierpiński gasket case: $\mathcal{T}^\infty$ depends non-trivially on the choice of a sequence ω in its definition, and different sequences typically give rise to non-isometric gaskets, with the boundary of $\mathcal{T}^\infty$ empty if and only if ω is eventually constant ([7], Lemma 5.1). The spectrum $\sigma(-\Delta_{\mathcal{T}^\infty})$, however, is independent of

ω (even if the spectral decomposition is not, see Remark 5.4 in [7] or Proposition 1 in [4]). Using the notation

$$\mathcal{R}(z) = \lim_{n\to\infty} 5^n (S_{-1,\mathcal{T}})^n(z),$$

we have the following result on the spectrum $\sigma(-\Delta_{\mathcal{T}^\infty})$.

Proposition 3 ([7], Theorem 4)**.** *The operator $-\Delta_{\mathcal{T}^\infty}$ is an unbounded self-adjoint operator from a dense domain in $L^2(\mathcal{T}^\infty, \mu^\infty)$ to $L^2(\mathcal{T}^\infty, \mu^\infty)$. Its spectrum is $\sigma(-\Delta_{\mathcal{T}^\infty}) = \mathcal{J}^\infty \cup \Sigma_3^\infty$ with*

$$\mathcal{J}^\infty = \bigcup_{n=-\infty}^{\infty} 5^n \mathcal{R}(\mathcal{J}_\mathcal{T}) \quad \textit{and} \quad \Sigma_3^\infty = \bigcup_{n=-\infty}^{\infty} 5^n \mathcal{R}(\Sigma_3),$$

where $\Sigma_3 = \bigcup_{n=0}^{\infty} R^{-n}(\{3\})$.

A number of generalizations of this result for other unbounded nested fractals have been proved, see, e.g., [17,18]. The proposition immediately yields the following corollary.

Corollary 2. *We have that* $\dim_H(\sigma(-\Delta_{\mathcal{T}^\infty})) = \dim_H(\mathcal{J}_\mathcal{T})$.

Thus, estimating the Hausdorff dimension of the spectrum $\sigma(-\Delta_{\mathcal{T}^\infty})$ is again equivalent to estimating the Hausdorff dimension of the Julia set $\mathcal{J}_\mathcal{T}$.

3. Related Results for Other Gaskets and Lattices

In this section, we describe other examples of fractal sets to which the same approach can be applied. In practice, the computations may be more complicated, but the same basic method still applies.

3.1. Higher-Dimensional Infinite Sierpiński Gaskets

Let $d \geqslant 2$ and $T_i \colon \mathbb{R}^d \to \mathbb{R}^d$ be contractions defined by

$$T_i(x_1, \ldots, x_d) = \left(\frac{x_1}{2}, \ldots, \frac{x_d}{2}\right) + \frac{1}{2} e_i, \quad \text{for } i = 1, \ldots, d,$$

where e_i is the ith coordinate vector. The d-dimensional Sierpiński gasket $\mathcal{T}^d \subset \mathbb{R}^d$ is the smallest non-empty closed set such that

$$\mathcal{T}^d = \bigcup_{i=1}^{d} T_i(\mathcal{T}^d).$$

In [3], the analogous results are presented for the spectrum of the Laplacian $\Delta_{\mathcal{T}^d}$ associated with the corresponding Sierpiński gasket $\mathcal{T}^d \subset \mathbb{R}^d$ in d dimensions ($d \geqslant 3$).

Definition 10. *For a sequence $(\omega_n)_{n\in\mathbb{N}} \subset \{1, \ldots, d\}^{\mathbb{N}}$ we can define an infinite Sierpiński gasket in d dimensions as*

$$\mathcal{T}^{d,\infty} = \bigcup_{n=1}^{\infty} T_{\omega_1}^{-1} \circ \cdots \circ T_{\omega_n}^{-1}(\mathcal{T}^d).$$

As before, we can associate a Julia set $\mathcal{J}_{\mathcal{T}^d}$ and consider its Hausdorff dimension $\dim_H(\mathcal{J}_{\mathcal{T}^d})$. More precisely, in each case, we can consider the decimation polynomial $R_{\mathcal{T}^d} \colon [0, 3+d] \to \mathbb{R}$ defined by

$$R_{\mathcal{T}^d}(x) = x((3+d) - x),$$

with two local inverses $S_{\pm 1,\mathcal{T}^d}\colon [0,3+d] \to [0,3+d]$ given by

$$S_{\epsilon,\mathcal{T}^d}(x) = \frac{1}{2}\left(3+d+\epsilon\sqrt{9+6d+d^2-4x}\right) \quad \text{with } \epsilon = \pm 1.$$

Let $\mathcal{J}_{\mathcal{T}^d} \subset [0,3+d]$ be the limit set of these two contractions, i.e., the smallest non-empty closed set such that

$$\mathcal{J}_{\mathcal{T}^d} = S_{-1,\mathcal{T}^d}(\mathcal{J}_{\mathcal{T}^d}) \cup S_{+1,\mathcal{T}^d}(\mathcal{J}_{\mathcal{T}^d}).$$

Theorem 2. *The Hausdorff dimension* $\dim_H(\mathcal{J}_{\mathcal{T}^d})$ *of the Julia set* $\mathcal{J}_{\mathcal{T}^d}$ *for* $d \in \{2,\dots,10\}$ *associated with the Sierpiński gasket in d dimensions is given by the values in Table 1, accurate to the number of decimals stated.*

Table 1. The Hausdorff dimension of $\mathcal{J}_{\mathcal{T}^d}$ for $2 \leqslant d \leqslant 10$.

d	$\dim_H(\mathcal{J}_{\mathcal{T}^d})$
2	0.55161856837246 …
3	0.45183750018171 …
4	0.39795943979056 …
5	0.36287714809375 …
6	0.33770271892130 …
7	0.31850809575800 …
8	0.30324865557723 …
9	0.29074069840192 …
10	0.28024518050407 …

The proof uses the same algorithmic method as that of Theorem 1, see Section 4.

Remark 4. *By arguments developed in [1,4], one can deduce that similarly to Proposition 3 and Corollary 2, the Hausdorff dimensions of the spectrum of the appropriately defined Laplacian on* $\mathcal{T}^{d,\infty}$ *and the Julia set* $\dim_H(\mathcal{J}_{\mathcal{T}^d})$ *coincide.*

We can observe empirically from the table that the dimension decreases as $d \to +\infty$. The following simple lemma confirms that $\lim_{d\to+\infty} \dim_H(\mathcal{J}_{\mathcal{T}^d}) = 0$ with explicit bounds.

Lemma 2. *As* $d \to +\infty$ *we can bound*

$$\frac{\log 2}{\log(d+3)} \leqslant \dim_H(\mathcal{J}_{\mathcal{T}^d}) \leqslant \frac{2\log 2}{\log(d+3)+\log(d-1)}.$$

Proof. We can write

$$I_1 := R^{-1}_{\mathcal{T}^d}([0,3+d]) \cap \left[0,\frac{3+d}{2}\right] = \left[0,\frac{3+d}{2}\left(1-\sqrt{1-\frac{4}{3+d}}\right)\right].$$

Thus, for $x \in I_1$ we have bounds

$$\sqrt{(3+d)(d-1)} \leqslant |R'_{\mathcal{T}^d}(x)| \leqslant 3+d.$$

Similarly, we can define $I_2 := R^{-1}_{\mathcal{T}^d}([0,3+d]) \cap \left[\frac{3+d}{2},3+d\right]$ and obtain the same bounds on $|R'_{\mathcal{T}^d}(x)|$ for $x \in I_2$. In particular, we can then bound

$$\frac{\log 2}{\log(3+d)} \leqslant \dim_H(\mathcal{J}_{\mathcal{T}^d}) \leqslant \frac{2\log 2}{\log(3+d)+\log(d-1)}. \quad \square$$

3.2. Post-Critically Finite Self-Similar Sets

The method of spectral decimation used for the Sierpiński gasket by Fukushima and Shima [1], was extended by Shima [5] to post-critically finite self-similar sets and thus provided a method for analyzing the spectra of their Laplacians.

Definition 11. *Let* $\Sigma = \{1, \ldots, k\}^{\mathbb{Z}_+}$ *be the space of (one-sided) infinite sequences with the Tychonoff product topology, and* σ *the usual left-shift map on* Σ.

Let $T_1, \ldots, T_k \colon \mathbb{R}^d \to \mathbb{R}^d$ *be contracting similarities and let* $\mathcal{X}$ *be the limit set, i.e., the smallest closed subset with* $\mathcal{X} = \bigcup_{i=1}^{k} T_i(\mathcal{X})$. *Let* $\pi \colon \Sigma \to \mathcal{X}$ *be the natural continuous map defined by*

$$\pi((w_n)_{n=0}^{\infty}) = \lim_{n \to +\infty} T_{w_0} T_{w_1} \cdots T_{w_n}(0).$$

We say that $\mathcal{X}$ *is post-critically finite if*

$$\#\left(\bigcup_{n=0}^{\infty} \sigma^n \{(w_n) \in \Sigma : \pi(w_n) \in K\} \right) < +\infty$$

where $K = \bigcup_{i \neq j} T_i \mathcal{X} \cap T_j \mathcal{X}$.

The original Sierpiński triangle $\mathcal{T}$ is an example of a limit set which is post-critically finite. So is the following variant on the Sierpiński triangle.

Example 2 (SG_3 gasket)**.** *We can consider the Sierpiński gasket* SG_3 *(see Figure 5) which is the smallest non-empty closed set* $\mathcal{X}_{SG_3}$ *such that* $\mathcal{X}_{SG_3} = \bigcup_{i=1}^{6} T_i \mathcal{X}_{SG_3}$ *where*

$$T_j(x, y) = p_j + \left(\frac{x}{3}, \frac{y}{3}\right) \quad \text{for } j = 1, \ldots, 6,$$

with

$$p_1 = (0,0), p_2 = \left(\frac{1}{3}, 0\right), p_3 = \left(\frac{2}{3}, 0\right), p_4 = \left(\frac{1}{6}, \frac{1}{2\sqrt{3}}\right), p_5 = \left(\frac{1}{2}, \frac{1}{2\sqrt{3}}\right), p_6 = \left(\frac{1}{3}, \frac{1}{\sqrt{3}}\right).$$

In this case, we can associate the decimation rational function $R_{SG_3} \colon [0,6] \to [0,6]$ *given by*

$$R_{SG_3}(x) = \frac{3x(5-x)(4-x)(3-x)}{14-2x},$$

for which there are four local inverses S_{j,SG_3} *(for* $j = 1, 2, 3, 4$*) [19], see Figure 6. The associated Julia set* $\mathcal{J}_{SG_3}$*, which is the smallest non-empty closed set such that* $\mathcal{J}_{SG_3} = \bigcup_{j=1}^{4} S_{j,SG_3}(\mathcal{J}_{SG_3})$*, has Hausdorff dimension* $\dim_H(\mathcal{J}_{SG_3})$.

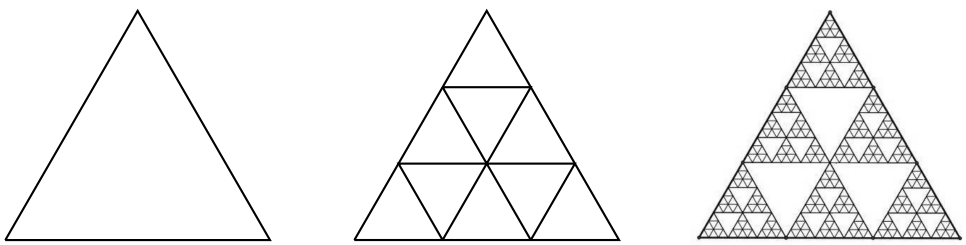

X_0 X_1

Figure 5. The first two graphs for SG_3 (**left**, **centre**) and the SG_3 gasket (**right**).

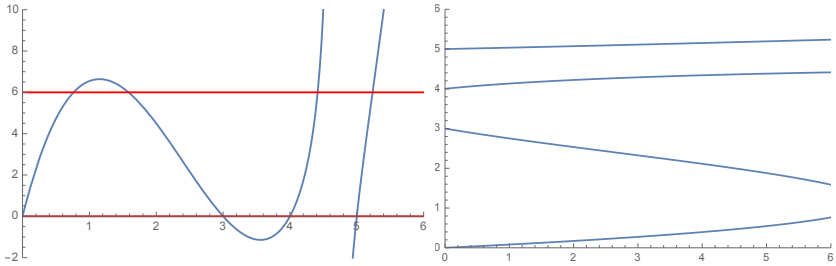

Figure 6. The function $R_{SG_3}(x)$ and the four contracting inverse branches for the SG_3 gasket.

Using Mathematica with a sufficiently high precision setting (see Example 5 for more details), we can numerically compute the Hausdorff dimension of the Julia set $\mathcal{J}_{SG_3}$ associated with the Sierpiński gasket SG_3 to be

$$\dim_H(\mathcal{J}_{SG_3}) = 0.617506301862352229042494874316407096341976\ldots$$

Example 3 (Vicsek graph). *The Vicsek set $X_{\mathcal{V}}$ is the smallest non-empty closed set such that $X_{\mathcal{V}} = \bigcup_{j=1}^{5} T_j(X_{\mathcal{V}})$ where*

$$T_j(x,y) = p_j + \left(\frac{x}{3}, \frac{y}{3}\right) \quad \text{for } j = 1,\ldots,5,$$

with

$$p_1 = (0,0),\ p_2 = \left(\frac{2}{3}, 0\right),\ p_3 = \left(\frac{2}{3}, \frac{2}{3}\right),\ p_4 = \left(0, \frac{2}{3}\right),\ p_5 = \left(\frac{1}{3}, \frac{1}{3}\right).$$

In this case, studied in [20], Example 6.3, one has that $R_{\mathcal{V}}\colon [-1,0] \to \mathbb{R}$ is given by

$$R_{\mathcal{V}}(z) = z(6z+3)(6z+5),$$

with three inverse branches $S_1, S_2, S_3\colon [-1,0] \to [-1,0]$ given by

$$S_1(x) = \frac{1}{36}\left(i(\sqrt{3}+i)t(x) - \frac{19(1+i\sqrt{3})}{t(x)} - 16\right),$$
$$S_2(x) = \frac{1}{36}\left(-i(\sqrt{3}-i)t(x) - \frac{19(1-i\sqrt{3})}{t(x)} - 16\right),$$
$$S_3(x) = \frac{1}{18}\left(t(x) + \frac{19}{t(x)} - 8\right),$$

where $t(x) = \left(9\cdot(81x^2+56x-75)^{1/2} + 81x + 28\right)^{1/3}$. The associated Julia set $\mathcal{J}_{\mathcal{V}}$ is the smallest non-empty closed set such that $\mathcal{J}_{\mathcal{V}} = \bigcup_{j=1}^{3} S_{j,\mathcal{V}}(\mathcal{J}_{\mathcal{V}})$. The following theorem is proved similarly to Theorem 1, as described in Section 4.

Theorem 3. *The Hausdorff dimension of the Julia set $\mathcal{J}_{\mathcal{V}}$ is*

$$\dim_H(\mathcal{J}_{\mathcal{V}}) = 0.49195457005266\ldots,$$

accurate to the number of decimals stated.

Remark 5. *Analogously to the case of the Sierpiński lattice $\mathcal{L}$, we can define lattices $\mathcal{L}_{SG_3}$ and $\mathcal{L}_{\mathcal{V}}$ for the SG_3 and Vicsek sets from the previous two examples, as well as corresponding graph Laplacians $\Delta_{\mathcal{L}_{SG_3}}$ and $\Delta_{\mathcal{L}_{\mathcal{V}}}$. The Hausdorff dimensions of their spectra can again be directly related to those of the respective Julia sets $\mathcal{J}_{SG_3}$ and $\mathcal{J}_{\mathcal{V}}$. By Theorem 5.8 in [20], one has that $\mathcal{J}_{SG_3} \subseteq \sigma(-\Delta_{\mathcal{L}_{SG_3}}) \subseteq \mathcal{J}_{SG_3} \cup \mathcal{D}_{SG_3}$ and $\mathcal{J}_{\mathcal{V}} \subseteq \sigma(-\Delta_{\mathcal{L}_{\mathcal{V}}}) \subseteq \mathcal{J}_{\mathcal{V}} \cup \mathcal{D}_{\mathcal{V}}$, where $\mathcal{D}_{SG_3}$ and $\mathcal{D}_{\mathcal{V}}$ are*

countable sets. It follows, analogously to Corollary 1, that $\dim_H(\sigma(-\Delta_{\mathcal{L}_{SG_3}})) = \dim_H(\mathcal{J}_{SG_3})$ *and* $\dim_H(\sigma(-\Delta_{\mathcal{L}_V})) = \dim_H(\mathcal{J}_V)$.

Remark 6. *Other examples to which the same method could be applied include the modified Koch curve (see [21,22]) for which the associated rational function is* $R(x) = 9x(x-1)(x-\frac{4}{3})(x-\frac{5}{3})/(x-\frac{3}{2})$. *More families of such examples can be found in [23].*

Remark 7. *The spectral decimation method can also apply to some non-post-critically finite examples, such as the diamond fractal [24], for which the associated polynomial is* $R(x) = 2x(2+x)$. *On the other hand, there are symmetric fractal sets which do not admit spectral decimation, such as the pentagasket, as studied in [25].*

4. Dimension Estimate Algorithm for Theorem 1

This section is dedicated to finishing the proof of Theorem 1, by describing an algorithm yielding estimates (with rigorous error bounds) for the values of the Hausdorff dimension.

By the above discussion, we have reduced the estimation of the Hausdorff dimensions of $\sigma(-\Delta_{\mathcal{L}})$ and $\sigma(-\Delta_{\mathcal{T}^\infty})$ to that of $\dim_H(\mathcal{J}_{\mathcal{T}})$ for the limit set $\mathcal{J}_{\mathcal{T}}$ associated with $S_{\pm 1,\mathcal{T}}$ from (4) (and similarly for the other examples). Unfortunately, since the maps $S_{\pm 1,\mathcal{T}}$ are non-linear, it is not possible to give an explicit closed form for the value $\dim_H(\sigma(-\Delta_{\mathcal{T}})) = \dim_H(\mathcal{J}_{\mathcal{T}})$. Recently developed simple methods make the numerical estimation of this value relatively easy to implement, which we summarize in the following subsections.

4.1. A Functional Characterization of Dimension

Let $\mathcal{B} = C(I)$ be the Banach space of continuous functions on the interval $I = [0,5]$ with the norm $\|f\|_\infty = \sup_{x\in I} |f(x)|$.

Definition 12. *Let* $\mathcal{L}_t$ *(for* $t \geqslant 0$*) be the* transfer operator *defined by*

$$\mathcal{L}_t f(x) = |S'_{-1,\mathcal{T}}(x)|^t f(S_{-1,\mathcal{T}}(x)) + |S'_{+1,\mathcal{T}}(x)|^t f(S_{+1,\mathcal{T}}(x))$$

where $f \in \mathcal{B}$ *and* $x \in I$, *and* $S_{\pm 1,\mathcal{T}}$ *are as in* (4).

It is well known that the transfer operator $\mathcal{L}_t$ (for $t \geqslant 0$) is a well-defined positive bounded operator from $\mathcal{B}$ to itself. To make use of the results in the previous sections, we employ the following "min-max method" result:

Lemma 3 ([26]). *Given choices of* $0 < t_0 < t_1 < 1$ *and strictly positive continuous functions* $f, g\colon I \to \mathbb{R}^+$ *with*

$$\inf_{x\in I} \frac{\mathcal{L}_{t_0} f(x)}{f(x)} > 1 \quad \text{and} \quad \sup_{x\in I} \frac{\mathcal{L}_{t_1} g(x)}{g(x)} < 1, \tag{7}$$

then $t_0 < \dim_H(\mathcal{J}_{\mathcal{T}}) < t_1$.

Proof. We briefly recall the proof. We require the following standard properties.

1. For any $t \geqslant 0$ the operator $\mathcal{L}_t$ has a maximal positive simple eigenvalue $e^{P(t)}$ (with positive eigenfunction), where P is the pressure function [27,28].
2. $P\colon \mathbb{R}^+ \to \mathbb{R}$ is real analytic and convex [28].
3. The value $t = \dim(\mathcal{J}_{\mathcal{T}})$ is the unique solution to $P(t) = 0$, see [29,30].

By property 1. and the first inequality in (7), we can deduce that

$$P(t_0) = \lim_{n\to+\infty} \frac{1}{n} \log \|\mathcal{L}^n_{t_0} f\|_\infty > 0. \tag{8}$$

By property 1. and the second inequality in (7), we can deduce that

$$P(t_1) = \lim_{n\to+\infty} \frac{1}{n} \log \|\mathcal{L}_{t_1}^n g\|_\infty < 0. \tag{9}$$

Comparing properties 2. and 3. with (8) and (9), the result follows. □

4.2. Rigorous Verification of Minmax Inequalities

Next, we explain how we rigorously verify the conditions of Lemma 3 for a function $f\colon I \to \mathbb{R}^+$, that is,

1. $f > 0$;
2. $\inf_{x\in I} h(x) > 1$ or $\sup_{x\in I} h(x) < 1$ for $h(x) := (\mathcal{L}_t f)(x)/f(x)$.

In order to obtain rigorous results, we make use of the arbitrary precision ball arithmetic library Arb [31], which for a given interval $[c-r, c+r]$ and function f outputs an interval $[c'-r', c'+r']$ such that $f([c-r, c+r]) \subseteq [c'+r', c'-r']$ is guaranteed. Clearly, the smaller the size of the input interval, the tighter the bounds on its image. Thus, in order to verify the above conditions, we partition the interval I adaptively using a bisection method up to depth $k \in \mathbb{N}_0$ into at most 2^k subintervals, and verify these conditions on each subinterval. While the first condition is often immediately satisfied for chosen test functions f on the whole interval I, the second condition is much harder to verify as h is very close to 1 and would require very large depth k.

To counteract the exponential growth of the number of required subintervals, we use tighter bounds on the image of h. Clearly for $x \in [c-r, c+r]$ with $c \in \mathbb{R}$ and $r > 0$, we have that $|h(x) - h(c)| \leqslant \sup_{y\in[c-r,c+r]} |h'(y)|r$ by the mean value theorem. More generally, we obtain for $p \in \mathbb{N}$ that

$$|h(x) - h(c)| \leqslant \sum_{i=1}^{p-1} |h^{(i)}(c)|r^i + \sup_{y\in[c-r,c+r]} |h^{(p)}(y)|r^p.$$

This makes it possible to achieve substantially tighter bounds on $h([c-r, c+r])$ while using a moderate number of subintervals, at the cost of additionally computing the first p derivatives of h.

4.3. Choice of f and g via an Interpolation Method

Here, we explain how to choose suitable functions f and g for use in Lemma 3, so that given candidate values $t_0 < t_1$ we can confirm that $t_0 < \dim_H(\mathcal{J}_\mathcal{T}) < t_1$. Clearly, if f and g are eigenfunctions of $\mathcal{L}_{t_0}$ and $\mathcal{L}_{t_1}$ for the eigenvalues λ_{t_0} and λ_{t_1}, respectively, then condition (3) is easy to verify. As these eigenfunctions are not known explicitly, we will use the Lagrange–Chebyshev interpolation method to approximate the respective transfer operators by finite-rank operators of rank m, and thus obtain approximations $f^{(m)}$ and $g^{(m)}$ of f and g. As the maps $S_{\pm1,\mathcal{T}}$ involved in the definition of the transfer operator (Definition 12) extend to holomorphic functions on suitable ellipses, Theorem 3.3 and Corollary 3 of [32] guarantee that the (generalized) eigenfunctions of the finite-rank operator converge (in supremum norm) exponentialy fast in m to those of the transfer operator. In particular, for large enough m, the functions $f^{(m)}$ and $g^{(m)}$ are positive on the interval I and are good candidates for Lemma 3.

Initial choice of m. We first make an initial choice of $m \geqslant 1$. Let $\ell_n\colon I \to \mathbb{R}$ (for $n = 0, \dots, m-1$) denote the Lagrange polynomials scaled to $[0, 5]$ and let $x_n \in [0, 5]$ (for $n = 0, \dots, m-1$) denote the associated Chebyshev points.

Initial construction of test functions. Let $v^t = (v_i^t)_{i=0}^{m-1}$ be the left eigenvector for the maximal eigenvalue of the $m \times m$ matrix $M_t(i, j) = (\mathcal{L}_t \ell_i)(x_j)$ (for $0 \leqslant i, j \leqslant m-1$) and set

$$f^{(m)} := \sum_{i=0}^{m-1} v_i^{t_0} \ell_i \quad \text{and} \quad g^{(m)} := \sum_{i=0}^{m-1} v_i^{t_1} \ell_i.$$

A fast practical implementation of this requires a slight variation (see Algorithm 1 in [32]), which can be implemented using a discrete cosine transform.

If the choices $f = f^{(m)}$ and $g = g^{(m)}$ satisfy the hypotheses of Lemma 3 (which can be verified rigorously with the method in the previous section), then we proceed to the next step. If they do not, we increase m and try again.

Conclusion. When the hypothesis of Lemma 3 holds, then its assertion confirms that $t_0 < \dim_H(\mathcal{J}_\mathcal{T}) < t_1$.

It remains to iteratively make the best possible choices of $t_0 < t_1$ using the following approach.

4.4. The Bisection Method

Fix $\epsilon > 0$. We can combine the above method of choosing f and g with a bisection method to improve given lower and upper bounds t_0 and t_1 until the latter are ϵ-close:

Initial choice. First, we can set $t_0^{(1)} = 0$ and $t_1^{(1)} = 1$, for which $t_0^{(1)} < \dim_H(\mathcal{J}_\mathcal{T}) < t_1^{(1)}$ is trivially true.

Iterative step. Given $n \geqslant 0$, we assume that we have chosen $t_0^{(n)} < t_1^{(n)}$. We can then set $T = (t_0^{(n)} + t_1^{(n)})/2$ and proceed as follows.

(i) If $t_0^{(n)} < \dim_H(\mathcal{J}_\mathcal{T}) < T$ then set $t_0^{(n+1)} = t_0^{(n)}$ and $t_1^{(n+1)} = T$.
(ii) If $T < \dim_H(\mathcal{J}_\mathcal{T}) < t_1^{(n)}$ then set $t_0^{(n+1)} = T$ and $t_1^{(n+1)} = t_1^{(n)}$.
(iii) If $\dim_H(\mathcal{J}_\mathcal{T}) = T$ then we have the final value (in practical implementation, this case is of no relevance, and the only meaningful termination condition is given by $t_1 - t_0 < \epsilon$).

Final choice. Once we arrive at $t_1^{(n)} - t_0^{(n)} < \epsilon$ then we can set $t_0 = t_0^{(n)}$ and $t_1 = t_1^{(n)}$ as the resulting upper and lower bounds for the true value of $\dim_H(\mathcal{J}_\mathcal{T})$.

Applying this algorithm yields the proof of Theorem 1 (and with the obvious modifications also those of Theorems 2 and 3). Specifically, we computed the value of $\dim_H(\mathcal{J}_\mathcal{T})$ efficiently to the 14 decimal places as stated by the above method, by setting $\epsilon = 10^{-15}$, using finite-rank approximation up to rank $m = 30$, running interval bisections for rigorous minmax inequality verification up to depth $k = 18$, i.e., using up to 2^{18} subintervals, and using $p = 2$ derivatives. There are of course many ways to further improve accuracy, e.g., with more computation or the use of higher derivatives.

Example 4 (Sierpiński triangle)**.** *To cheaply obtain a more accurate estimate (albeit without the rigorous guarantee resulting from the use of ball arithmetic), we use the* MaxValue *routine from Mathematica. To obtain an estimate on* $\dim_H(\mathcal{J}_\mathcal{T})$ *to* 60 *decimal places, we work with* 100 *decimal places as Mathematica's precision setting. Taking* $m = 60$*, we use the bisection method and starting from an interval* $[0.2, 0.8]$ *after* 199 *iterations we have upper and lower bounds* $t_0 \leqslant \dim_H(\mathcal{J}_\mathcal{T}) \leqslant t_1$*, where*

$$t_0 = 0.551618568372460931697570872313520654536079741744042208266296600050480034158120334482826486939105470 5$$

and

$$t_1 = 0.551618568372460931697570872313520654536079741744042208266298093574146720832130049058199394168923212 2.$$

*With a little more computational effort (*200 *decimals of precision,* $m = 100$*,* 329 *iterations), we can improve the estimate to* 100 *decimal places:*

$$t_0 = 0.551618568372460931697570876084565434172117664507138868116831699168666814224190486583439508658139692480473399364569014861603996382396316337795734913712923897955012169395005328912685736846989079087113344$$

and

$$t_1 = 0.55161856837246093169757087608456543417211766450713$$
$$88681168316991686668142241904865834395086581396926$$
$$63351381969733012016129364111250869850101334085360$$
$$70969237514708581622707399079704491867257671463809,$$

which yields the estimate:

$$\dim_H(\mathcal{J}_{\mathcal{T}}) = 0.55161856837246093169757087608456543417211766$$
$$450718868116831699168666814224190486583439508658139692\ldots.$$

We next consider as a second example, SG_3, see Example 2.

Example 5 (SG_3 gasket)**.** *With the same method as in the previous example, we estimate bounds on* $\dim_H(\mathcal{J}_{SG_3})$ *to* 60 *decimal places:*

$$t_0 = 0.61750630186235222904249487431640709634197686636096160395161406191565986666910504993567729050418757 73$$

and

$$t_1 = 0.61750630186235222904249487431640709634197686636096160395161519347588053917619434982903347584784816 58,$$

which yields the estimate:

$$\dim_H(\mathcal{J}_{SG_3}) = 0.61750630186235222904249487431640709634197686636096160395161\ldots$$

Remark 8. *A significant contribution to the time complexity of the algorithm is that of estimating the top eigenvalue and corresponding eigenvector of an* $m \times m$ *matrix which is* $O(n \cdot m^2)$ *with* n *denoting the number of steps of the power iteration method. Moreover, by the perturbation theory one may expect that, in order to obtain an error in the eigenvector of* $\epsilon > 0$*, one needs to choose* $m = O(\log(1/\epsilon))$ *and* $n = O(\log(1/\epsilon))$*.*

5. Conclusions

In this work, we have leveraged the existing theory on Laplacians associated to Sierpiński lattices, infinite Sierpiński gaskets and other post-critically finite self-similar sets, in order to establish the Hausdorff dimensions of their respective spectra. We used the insight that, by virtue of the iterative description of these spectra, these dimensions coincide with those of the Julia sets of certain rational functions. Since the contractive local inverse branches of these functions are non-linear, the values of the Hausdorff dimensions are not available in an explicit closed form, in contrast to the dimensions of the (infinite) Sierpiński gaskets themselves, or other self-similar fractals constructed using contracting similarities and satisfying an open set condition. Therefore, we use the fact that the Hausdorff dimension can be expressed implicitly as the unique zero of a so-called pressure function, which itself corresponds to the maximal positive simple eigenvalue of a family of positive transfer operators. Using a min-max method combined with the Lagrange–Chebyshev interpolation scheme, we can rigorously estimate the leading eigenvalues for every operator in this family. Combined with a bisection method, we then accurately and efficiently estimate the zeros of the respective pressure functions, yielding rigorous and effective bounds on the Hausdorff dimensions of the spectra of the relevant Laplacians.

Author Contributions: Conceptualization, M.P. and J.S. All authors have read and agreed to the published version of the manuscript.

Funding: The authors were partly supported by ERC-Advanced Grant 833802-Resonances.

Data Availability Statement: Not applicable.

Conflicts of Interest: The authors declare no conflict of interest.

References

1. Fukushima, M.; Shima, T. On a spectral analysis for the Sierpiński gasket. *Potential Anal.* **1992**, *1*, 1–35. [CrossRef]
2. Kigami, J. *Analysis on Fractals*; Cambridge Tracts in Mathematics 143; Cambridge University Press: Cambridge, UK, 2008.
3. Rammal, R. Spectrum of harmonic excitations on fractals. *J. Phys.* **1984**, *45*, 191–206. [CrossRef]
4. Sabot, C. Laplace operators on fractal lattices with random blow-ups. *Potential Anal.* **2004**, *20*, 177–193. [CrossRef]
5. Shima, T. On eigenvalue problems for Laplacians on p.c.f. self-similar sets. *Jpn. J. Indust. Appl. Math.* **1996**, *13*, 1–23. [CrossRef]
6. Strichartz, R. Analysis on Fractals. *Not. Am. Math. Soc.* **1999**, *46*, 1199–1208.
7. Teplyaev, A. Spectral analysis on infinite Sierpiński gaskets. *J. Funct. Anal.* **1998**, *159*, 537–567. [CrossRef]
8. Falconer, K. *Fractal Geometry*; John Wiley & Sons: Chichester, UK, 2003.
9. Strichartz, R. *Differential Equations on Fractals: A Tutorial*; Princeton University Press: Princeton, NJ, USA, 2006.
10. Cohen, N. Fractal Antennas Part 1: Introduction and the Fractal Quad. *Commun. Q.* **1995**, *5*, 7–22.
11. Hohlfeld, R.; Cohen, N. Self-similarity and the geometric requirements for frequency independence in antennae. *Fractals* **1999**, *7*, 79–84. [CrossRef]
12. Kigami, J. A harmonic calculus on the Sierpinski spaces. *Jpn. J. Appl. Math.* **1989**, *8*, 259–290. [CrossRef]
13. Alexander, S. Some properties of the spectrum of the Sierpiński gasket in a magnetic field. *Phys. Rev. B* **1984**, *29*, 5504–5508. [CrossRef]
14. Rammal, R.; Toulouse, G. Random walks on fractal structures and percolation clusters. *J. Phys. Lett.* **1983**, *44*, 13–22. [CrossRef]
15. Béllissard, J. Renormalization group analysis and quasicrystals. *Ideas and Methods in Quantum and Statistical Physics (Oslo, 1988)*; Cambridge University Press: Cambridge, UK, 1992; pp. 118–148.
16. Quint, J.-F. Harmonic analysis on the Pascal graph. *J. Funct. Anal.* **2009**, *256*, 3409–3460. [CrossRef]
17. Sabot, C. Pure point spectrum for the Laplacian on unbounded nested fractals. *J. Funct. Anal.* **2000**, *173*, 497–524. [CrossRef]
18. Strichartz, R.; Teplyaev, A. Spectral analysis on infinite Sierpiński fractafolds. *J. Anal. Math.* **2012**, *116*, 255–297. [CrossRef]
19. Drenning, S.; Strichartz, R. Spectral decimation on Hambley's homogeneous hierarchical gaskets. *Ill. J. Math.* **2009**, *53*, 915–937. [CrossRef]
20. Malozemov, L.; Teplyaev, A. Self-similarity, operators and dynamics. *Math. Phys. Anal. Geom.* **2003**, *6*, 201–218. [CrossRef]
21. Malozemov, L. Spectral theory of the differential Laplacian on the modified Koch curve. In *Proceedings of the Geometry of the Spectrum: 1993 Joint Summer Research Conference on Spectral Geometry, 17–23 July 1993, University of Washington, Seattle, WA, USA*; American Mathematical Society: Providence, RI, USA, 1994; pp. 193–224.
22. Malozemov, L.; Teplyaev, A. Pure point spectrum of the Laplacians on fractal graphs. *J. Funct. Anal.* **1995**, *129*, 390–405. [CrossRef]
23. Teplyaev, A. Harmonic coordinates on fractals with finitely ramified cell structure. *Canad. J. Math.* **2008**, *60*, 457–480. [CrossRef]
24. Kigami, J.; Strichartz, R.S.; Walker, K.C. Constructing a Laplacian on the diamond fractal. *Experiment. Math.* **2001**, *10*, 437–448. [CrossRef]
25. Adams, B.; Smith, S.A.; Strichartz, R.S.; Teplyaev, A. The spectrum of the Laplacian on the pentagasket. In *Fractals in Graz*; Springer: Basel, Switzerland, 2001; pp. 1–24.
26. Pollicott, M.; Vytnova, P. Hausdorff dimension estimates applied to Lagrange and Markov spectra, Zaremba theory, and limit sets of Fuchsian groups. *Trans. Am. Math. Soc. B* **2022**, *9*, 1102–1159. [CrossRef]
27. Parry, W.; Pollicott, M. Zeta functions and the periodic orbit structure of hyperbolic dynamics. *Astérisque* **1990**, *188*, 1–256.
28. Ruelle, D. *Thermodynamic Formalism*; Addison-Wesley: Reading, MA, USA, 1978.
29. Bowen, R. Hausdorff dimension of quasi-circles. *Publ. Math. IHES* **1979**, *50*, 11–25. [CrossRef]
30. Ruelle, D. Repellers for real analytic maps. *Ergod. Theory Dynam. Syst.* **1982**, *2*, 99–107. [CrossRef]
31. Johansson, F. Arb: Efficient arbitrary-precision midpoint-radius interval arithmetic. *IEEE Trans. Comput.* **2017**, *66*, 1281–1292. [CrossRef]
32. Bandtlow, O.F.; Slipantschuk, J. Lagrange approximation of transfer operators associated with holomorphic data. *arXiv* **2020**, arXiv:2004.03534.